Development 136, 3143-3152 (2009) doi:10.1242/dev.031492

Extra-embryonic syndecan 2 regulates organ primordia migration and fibrillogenesis throughout the zebrafish embryo

Cammon B. Arrington[1] and H. Joseph Yost[2,*]

One of the first steps in zebrafish heart and gut organogenesis is the migration of bilateral primordia to the midline to form cardiac and gut tubes. The mechanisms that regulate this process are poorly understood. Here we show that the proteoglycan syndecan 2 (Sdc2) expressed in the extra-embryonic yolk syncytial layer (YSL) acts locally at the YSL-embryo interface to direct organ primordia migration, and is required for fibronectin and laminin matrix assembly throughout the embryo. Surprisingly, neither endogenous nor exogenous *sdc2* expressed in embryonic cells can compensate for knockdown of *sdc2* in the YSL, indicating that Sdc2 expressed in extra-embryonic tissues is functionally distinct from Sdc2 in embryonic cells. The effects of *sdc2* knockdown in the YSL can be rescued by extra-embryonic Sdc2 lacking an extracellular proteolytic cleavage (shedding) site, but not by extra-embryonic Sdc2 lacking extracellular glycosaminoglycan (GAG) addition sites, suggesting that distinct GAG chains on extra-embryonic Sdc2 regulate extracellular matrix assembly, cell migration and epithelial morphogenesis of multiple organ systems throughout the embryo.

KEY WORDS: Cardiac, Fibronectin, Gut, Heart, Proteoglycan, Syndecan, Zebrafish

INTRODUCTION

The heart and gut develop from bilateral precursors located in the lateral plate mesoderm (Brand, 2003; McFadden and Olson, 2002; Roberts, 2000; Zaffran and Frasch, 2002). These precursors migrate from the lateral edges of the embryo to the midline where they fuse to form the primitive cardiac and gut tubes. These tubes subsequently loop and coil along the left-right axis to form a multichambered heart and organs of the digestive system (Horne-Badovinac et al., 2003; Stainier, 2001; Stainier, 2005). In zebrafish, cardiac precursors migrate between the endoderm and the extra-embryonic yolk syncytial layer (YSL) towards the midline (Fig. 1A,B) and fuse to form an intermediate structure termed the cardiac cone (Glickman and Yelon, 2002; Stainier, 2001; Trinh and Stainier, 2004; Yelon et al., 1999). This intermediate structure then elongates to form the primitive heart tube (Holtzman et al., 2007; Rohr et al., 2006). Disruption of cardiac primordia migration can lead to the formation of two separate hearts, a condition known as cardia bifida (Alexander et al., 1998; Chen et al., 1996; Stainier et al., 1996; Yelon, 2001). Although less well studied, a similar process appears to occur during gut morphogenesis (Sakaguchi et al., 2006).

Endoderm, primitive endocardium and extracellular matrix are required for normal cardiac primordia migration. Cardia bifida occurs in chick embryos after the disruption of regions destined to become the ventral gut or yolk sac (Rosenquist, 1970). Zebrafish mutants such as *oep*, *fau*, *cas* (*sox32*) and *bon* (Alexander et al., 1999; Dickmeis et al., 2001; Kikuchi et al., 2000) that lack endoderm or have severe endodermal defects also manifest cardia bifida. Zebrafish *cloche* mutants lack endocardium and have markedly abnormal hearts due to impaired cardiac cone and primitive heart tube formation (Holtzman et al., 2007). Defective function of sphingosine 1-phosphate, a lipid mediator implicated in cell-extracellular matrix interactions (Kawahara et al., 2009; Kupperman et al., 2000; Matsui et al., 2007; Osborne et al., 2008), or loss of fibronectin, a major constituent of the extracellular matrix, also lead to cardia bifida (Linask and Lash, 1988; Sakaguchi et al., 2006; Trinh and Stainier, 2004).

Initiation of fibronectin fibrillogenesis partly depends on interactions between the cell-binding domain of fibronectin and cell surface integrins (Akiyama et al., 1989; Dzamba et al., 1994; Fogerty et al., 1990; Sechler et al., 1997; Wu et al., 1993). Although less well understood, fibronectin heparin-binding domains also appear to interact with glycosaminoglycans on cell surface proteoglycans to augment the interaction of cells with fibronectin (Bultmann et al., 1998; Christopher et al., 1997; Hocking et al., 1994; McDonald et al., 1987; Schwarzbauer, 1991; Whiteford et al., 2007; Woods et al., 1988). Cells that lack glycosaminoglycan synthesis cannot adhere normally to fibronectin or establish a fibronectin matrix (Chung and Erickson, 1997; LeBaron et al., 1988). Dominant-negative syndecan 2 (Sdc2), a transmembrane heparin sulfate proteoglycan, blocks fibronectin fibrillogenesis in CHO cells (Klass et al., 2000) and in *Xenopus* animal cap ectoderm (Kramer and Yost, 2002). Based on these findings, Sdc2 may play a role in organ primordia migration by augmenting cellular adhesion of fibronectin and regulating fibrillar organization (Carey, 1997; Woods and Couchman, 1998).

Here we explore early roles of Sdc2 in zebrafish development. In early development, before the migration of cardiac and gut primordia, we find functional differences between embryonic and extra-embryonic Sdc2. Knockdown of *sdc2* in the embryo alone does not alter heart or gut primordia migration, whereas knockdown of *sdc2* exclusively in the extra-embryonic YSL results in defective heart and gut primordia migration, loss of fibronectin fibrillogenesis throughout the embryo, and deficient basement membrane laminin assembly adjacent to cardiomyocyte and gut endoderm precursors. These defects can be rescued by YSL expression of wild-type Sdc2 or YSL expression of Sdc2 in which the proteoglycan shedding site has been mutated, but not by expression of Sdc2 in the embryo. We propose a model in which organ primordia migration is dependent upon extracellular matrix assembly that requires extra-embryonic Sdc2 and begins at the interface between embryonic and extra-embryonic tissues.

[1]Division of Pediatric Cardiology and [2]Department of Neurobiology and Anatomy, University of Utah, Salt Lake City, UT 84112, USA.

*Author for correspondence (jyost@genetics.utah.edu)

Accepted 16 July 2009

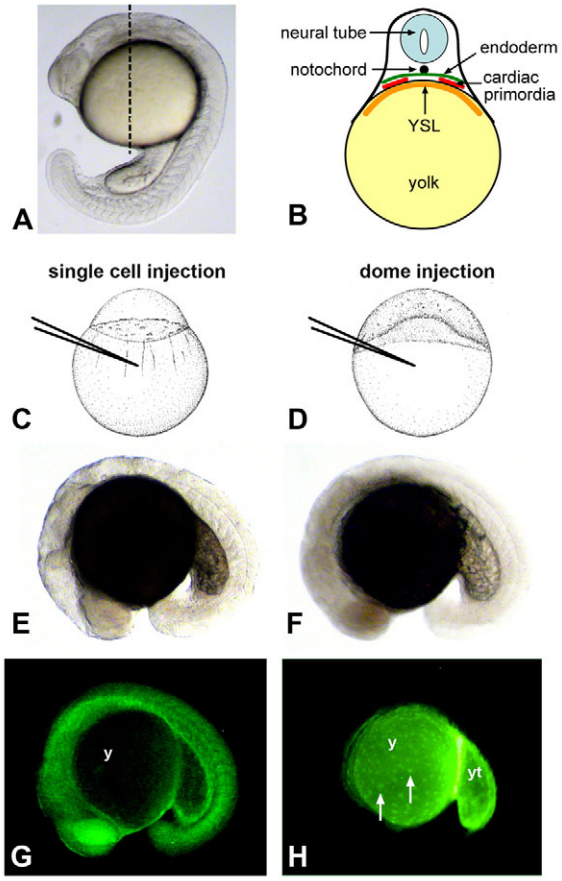

Fig. 1. Testing the role of embryonic and nonembryonic cell lineages in cardiac and gut morphogenesis. (**A**) Lateral view of a zebrafish embryo at the 21-somite stage. Dashed line represents the approximate anterior-posterior location of cardiac primordia at this stage. (**B**) Diagram represents a transverse section at the level of the dashed line shown in A. Cardiac precursors migrate between the endoderm and the extra-embryonic yolk syncytial layer (YSL) towards the midline. Early gut primordia are positioned analogously but are located posterior to the cardiac primordia. (**C**,**E**,**G**) Morpholino injection into an embryo at the 1-cell stage (C), and light (E) and fluorescent (G) microscopy of a traditional morphant at the 18-somite stage (lateral view). In single-cell injections, fluorescent morpholino is enriched in embryonic tissues and is significantly reduced in the yolk (y). (**D**,**F**,**H**) Morpholino injection into an embryo at the dome stage (D), and light (F) and fluorescent (H) microscopy of a yolk^{MO} embryo at the 18-somite stage (lateral view). In dome injections, fluorescent morpholino is restricted to the extra-embryonic yolk (y), posterior yolk tube (yt) and yolk syncytial nuclei (white arrows). Little, if any, fluorescence is detected within embryonic tissues.

MATERIALS AND METHODS

Zebrafish strains

Wild-type zebrafish (*Danio rerio*) embryos were obtained from crosses of Oregon AB fish. Zebrafish possessing green fluorescent hearts were derived from transgenic fish expressing a *cardiac myosin light chain 2:green fluorescent protein* fusion gene, *Tg(cmlc2:GFP)* (Huang et al., 2003). Endocardium was visualized using transgenic fish expressing a *friend leukemia integration 1:green fluorescent protein* fusion gene *Tg(fli1:GFP)* (Lawson and Weinstein, 2002). Embryos were maintained in embryo water between 24 and 28.5°C and staged according to age (hours post fertilization, hpf) and morphological criteria (Kimmel et al., 1995; Westerfield, 1994).

Injection of morpholino antisense oligonucleotides and synthesized mRNA

Morpholinos designed against *sdc2* were injected into the YSL at the dome stage (4.3 hpf). Either 16 ng/embryo of a splice-blocking morpholino, MO(SB) (5′-GTGATGCAGACGCTCACCTGATCCC-3′), or 8 ng/embryo of a translation-blocking morpholino, AUG(MO) (5′-ATCCAA-AGGTTCCTCATAATTCCTC-3′), were injected. Embryos were co-injected with 1-2 ng/embryo of rhodamine-conjugated control morpholino (5′-CCTCTTACCTCAGTTACAATTTATA-3′). Using a dissecting microscope with a rhodamine filter cube, embryos with a uniform distribution of injected material within the yolk and YSL were selected for further analysis. Capped sense *sdc2*, *GFP-sdc2*, *sdc2-hCD4JM* and *sdc2-ΔGAG* mRNA was synthesized using the mMESSAGE mMACHINE in vitro transcription kit (Ambion) and purified as described previously (Rupp et al., 1994). For mRNA rescue experiments, between 400 and 600 pg/embryo of *sdc2*, *sdc2-hCD4JM* and *sdc2-ΔGAG* mRNA was injected into the YSL at the dome stage. The *GFP-sdc2* construct was designed to detect proteolytic cleavage of the N-terminal ectodomain. In the *sdc2-hCD4JM* mRNA construct, the putative juxtamembrane cleavage sequence of Sdc2 (DPQDVQSENLFQRTE) was replaced with noncleavable sequence from human CD4 (VKVLPTWSTRVQPMA) (Wang et al., 2005). In the *sdc2-ΔGAG* construct, the N-terminal membrane localization sequence was retained but all GAG attachment serines were deleted. All morpholino and mRNA injections were repeated at least three times.

RT-PCR

For RT-PCR of *sdc2* cDNA, 50 wild-type and 50 *sdc2* MO-injected embryos were collected at the 21-somite stage and total RNA was isolated. RT-PCR reactions were performed using the SuperScript II RT-PCR Kit (Gibco BRL) with the *sdc2*-specific RT primer pair (5′-GACGACCTG-TACCTGGAGGA-3′ and 5′-GCTCTGCTTTAGGCACGAAG-3′) to amplify the *sdc2* cDNA fragments.

In situ hybridization

Digoxigenin-labeled antisense RNA probes were synthesized by in vitro transcription using T3, T7 and SP6 polymerases. cDNA templates used in this study included *cmlc2* (Yelon et al., 1999), *foxa3* (Odenthal and Nusslein-Volhard, 1998), *sdc2*, *sox17* (Alexander and Stainier, 1999), α_5 *integrin* (Koshida et al., 2005), β_1 *integrin* (*itgb1b*) (Mould et al., 2006) and *fibronectin 1* (Trinh and Stainier, 2004). Whole-mount in situ hybridization was carried out as described previously (Thisse et al., 1993) using a Biolane HTI in situ machine (Huller and Huttner AG, Tübingen, Germany). Embryos were cleared in 70% glycerol in PBST and photographed with a Leica MZ12 stereoscope using a Dage-MTI DC330 CCD camera.

Immunohistochemistry

Embryos were fixed overnight in a 50:50 mixture of 8% paraformaldehyde:1× PBS at 4°C and were dehydrated stepwise into methanol for storage at –20°C. After stepwise rehydration, embryos were manually deyolked and blocked for 1 hour in PBDT (1% BSA, 1% DMSO, 0.1% Triton X-100 in PBS pH 7.3). The deyolked embryos were embedded in 4% low-melt agarose and were sectioned using a vibratome (Electron Microscopy Sciences, OTS-3000). Primary antibodies used in this study included: rabbit polyclonal anti-fibronectin antibody (1:200; Sigma, F3648), rabbit polyclonal anti-laminin (1:200; Sigma, L9393), rabbit polyclonal anti-aPKC (1:200; Santa Cruz Biotechnology, sc-216), mouse IgG anti-β-catenin (1:400; BD Transduction Laboratories, 610153), mouse IgG2 anti-GFP (1:300; Living Colors Monoclonal Antibody JL-8; Clontech, 632381). Alexa Fluor antibodies (Molecular Probes) were used as secondary antibodies at a concentration of 1:300. Sections were equilibrated in SlowFade Antifade buffer (Molecular Probes, 2828) and mounted on microscope slides for imaging. Embryo sections were imaged using an Olympus FluoView scanning laser confocal microscope with a 60× objective. To ensure consistent adjustment of microscope power and gain settings, wild-type embryos were imaged in all experiments.

Western blot

Protein lysates were made from 50 dechorionated embryos at the 21-somite stage (19.5 hpf) that were placed in 1 ml deyolking buffer (55 mM NaCl, 1.8 mM KCl, 1.25 mM $NaHCO_3$). Yolk sacs were disrupted by pipetting with a 200 μl tip. The embryos were shaken for 5 minutes at 300 rpm to dissolve the yolk. Cells were pelleted at 300 ***g*** for 30 seconds and the supernatant was discarded. Two additional wash steps were performed by adding 1 ml wash buffer (110 mM NaCl, 3.5 mM KCl, 2.7 mM $CaCl_2$, 10 mM TrisHCl pH 8.5), shaking and pelleting cells as before. The pelleted cells were dissolved in 2 μl 2× SDS sample buffer per embryo and incubated for 5 minutes at 95°C. Samples were loaded on an 8% SDS-polyacrylamide gel (ten embryos per lane) and transferred to a PVDF membrane. Immunoblotting was performed using rabbit polyclonal anti-fibronectin antibody (1:3000; Sigma, F3648) followed by HRP anti-rabbit IgG (1:6000, Cell Signaling, #7074). The membrane was developed using ECL Plus and chemifluorescence was measured using a Storm scanner (GE Healthcare, Piscataway, NJ, USA).

RESULTS

Targeted gene knockdown in zebrafish nonembryonic yolk cells

sdc2 is expressed ubiquitously during early development in zebrafish, including strong expression in extra-embryonic yolk syncytial layer (YSL) nuclei (Fig. 2A). During gastrulation, YSL nuclei accumulate within the cortical cytoplasm of the yolk as marginal blastomeres collapse onto the yolk cell (D'Amico and Cooper, 2001; Kimmel and Law, 1985). The YSL has been implicated in mesoderm induction (Chen and Kimelman, 2000; Ober and Schulte-Merker, 1999), axial patterning via Wnt and Nodal cell signaling pathways (Bischof and Driever, 2004), and migration of cardiac primordia (Kawahara et al., 2009; Sakaguchi et al., 2006). Here, we explore the function of extra-embryonic YSL-expressed *sdc2* by morpholino knockdown and compare this with the knockdown of *sdc2* in embryonic cells.

Most morpholino-based gene knockdown studies in zebrafish involve injection at the 1-to-2-cell stage, allowing gene knockdown in all embryonic cells during early development (Nasevicius and Ekker, 2000). It is not widely appreciated that morpholinos injected at this stage, even when injected into the yolk cell, are predominantly swept into early cleavage blastomeres (Fig. 1C,E,G). Efficient morpholino uptake into embryonic cells is likely to be driven by microtubule-dependent cytoplasmic streaming that occurs during the first few cell cycles. Cytoplasmic bridges allow small molecules, including morpholinos, to pass from the yolk cell to marginal blastomeres until the sphere stage (4 hpf) (Amack and Yost, 2004). In order to target morpholinos exclusively to the yolk, embryos were injected slightly later, at the dome stage (4.3 hpf). Fluorescent morpholinos injected at the dome stage were detected by fluorescence in the yolk, yolk syncytial nuclei and posterior yolk tube, but not in embryonic cells (Fig. 1D,F,H). Hereafter, we refer to such embryos as yolk^{MO} embryos, to distinguish them from traditional morphant embryos injected at the 1-to-2-cell stage, in which morpholinos are mainly localized to embryonic tissues and are largely excluded from the yolk.

The yolk forms a functionally distinct compartment from the embryo. Despite ubiquitous expression of Sdc2 throughout early development, there were obvious phenotypic differences between traditional *sdc2* morphants and those injected with the *sdc2* morpholino at the dome stage (yolk^{sdc2MO} embryos). Yolk^{sdc2MO} embryos displayed a spectrum of cardiac and gut migration defects including cardia bifida and a bifid foregut, neither of which was observed in traditional morphants injected with either *sdc2* SB(MO) (*n*=221) or AUG(MO) (*n*=369). Instead, left-right patterning defects including reversed heart and gut looping were seen in traditional *sdc2* morphants (data not shown).

Sdc2 in YSL regulates heart and gut primordia migration

Using the yolk^{MO} technique described above, *sdc2* antisense morpholinos were injected into the yolk at the dome stage (4.3 hpf) to knock down *sdc2* exclusively in the YSL. Co-injection of a rhodamine-tagged control morpholino allowed visualization of the injected material and selection of embryos with a uniform distribution of morpholino within the yolk and YSL, with no morpholino in embryonic cells. Dome-stage injections of either translation-blocking or splice-blocking morpholinos resulted in the same phenotype, suggesting specific targeting of *sdc2* mRNA by these morpholinos. Additional evidence supporting morpholino efficacy comes from RT-PCR analysis of *sdc2* SB(MO)-injected embryos, in which *sdc2* RNA retained intron 2 (929 bp), which is predicted to cause premature translation termination (see Fig. S1 in the supplementary material).

Early in development (18-somite stage), the patterning in yolk^{sdc2MO} embryos was fairly normal (compare Fig. 2B and Fig. 2C), indicating that YSL-derived Sdc2 is not necessary for early functions, including mesoderm induction, gastrulation, and anterior-posterior and dorsal-ventral patterning. Later in development (40 hpf), yolk^{sdc2MO} embryos were smaller, with a defective posterior yolk tube and a correspondingly larger yolk cell (compare Fig. 2G and Fig. 2H). yolk^{sdc2MO} embryos also appeared to have decreased pigmentation and impaired migration of pigmented cells to the region immediately dorsal to the yolk tube.

Evaluation of heart formation by in situ hybridization using the cardiac-specific marker *cmlc2* (also known as *myl7*) revealed complete fusion of cardiac primordia in all wild-type control embryos by 20 hpf (22-somite stage, *n*=19). By contrast, over 67% (29/43) of yolk^{sdc2MO} embryos displayed defects in heart-field migration, 28% with incomplete heart-field fusion and 39% with persisting bilateral heart fields (Fig. 2D-F). Looping of the primitive heart tube is well underway by 40 hpf in wild-type embryos, but cardiac development was arrested in many yolk^{sdc2MO} embryos well before formation of the primitive heart tube. At 40 hpf, over 66% (179/270) of yolk^{sdc2MO} embryos displayed cardiac defects including impaired blood flow and pericardial edema, with pooling of blood around the heart field, and a spectrum of cardiac anomalies including a band-like distribution of myocardial cell precursors, cardia bifida, incomplete fusion of bilateral heart fields and impaired elongation of the cardiac cone to form the primitive heart tube (Fig. 2I). Using transgenic embryos, *Tg(cmlc2:GFP)* (Huang et al., 2003), we found that the aberrantly positioned cardiomyocytes were contractile and, in embryos with cardia bifida, two dysmorphic hearts beat independently (see Movie 1 in the supplementary material), demonstrating that other aspects of cardiac morphogenesis continue despite impaired cardiac primordia migration to the midline (Li et al., 2004).

To assess whether the phenotypes observed in yolk^{sdc2MO} embryos were specific to the function of Sdc2 and not the result of injecting morpholinos into the YSL, control experiments were performed in which 16 ng of either a rhodamine-conjugated control morpholino or a morpholino designed to knock down *spadetail* (*spt*, also known as *tbx16*) (Amack et al., 2007) was injected into each embryo at the dome stage. Yolk^{sptMO} embryos had normal cardiac primordia migration (*n*=26), as did yolk^{contMO} embryos (*n*=52). The only cardiac anomaly noted in these embryos was a 3-

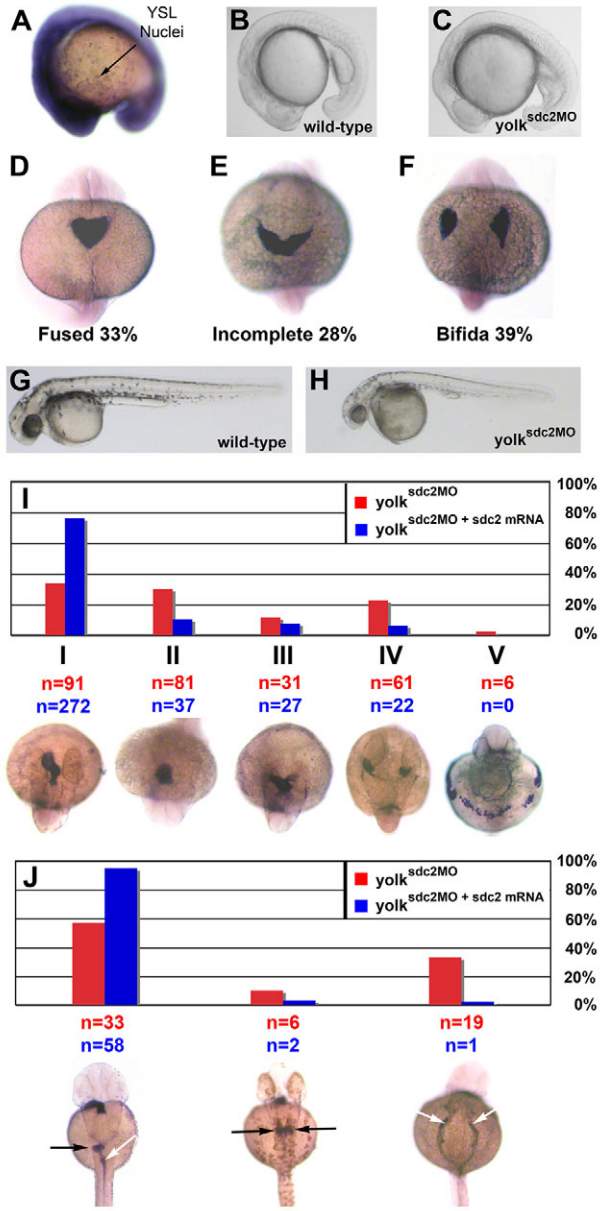

Fig. 2. Impaired cardiac primordia and primitive foregut migration in yolk^{sdc2MO} embryos. (**A**) Ubiquitous expression of *sdc2* at the 16-somite stage. Strong expression is seen throughout embryonic tissues and within individual yolk syncytial nuclei. (**B**,**C**) Lateral views of wild-type (B) and yolk^{sdc2MO} (C) embryos at the 18-somite stage. Patterning of yolk^{sdc2MO} embryos is relatively normal at this stage. (**D-F**) Expression of *cmlc2* in embryos at the 22-somite stage (dorsal view). Bilateral cardiac primordia were completely fused in 100% of wild-type embryos but only in 33% of yolk^{sdc2MO} embryos (D) at this stage. Cardiac primordia migration was defective in yolk^{sdc2MO} embryos, with 28% manifesting incomplete heart-field fusion (E) and 39% with cardia bifida (F). (**G**,**H**). Lateral views of wild-type (G) and yolk^{sdc2MO} (H) embryos at 40 hpf. The overall patterning in yolk^{sdc2MO} embryos remains normal, but the embryos are smaller, with a defective posterior yolk tube, larger yolk cell, pericardial edema and decreased pigmentation (H). (**I**) Bar graph depicting the spectrum of cardiac defects seen in yolk^{sdc2MO} embryos (red bars) and yolk^{sdc2MO} embryos co-injected with *sdc2* mRNA (blue bars) at 40 hpf. Below the graph, the expression of *cmlc2* is shown in embryos displaying the spectrum of cardiac phenotypes seen in yolk^{sdc2MO} embryos (dorsal view, anterior up for class I-IV embryos; ventral view, anterior up for class V embryo). Cardiac phenotypes vary in severity from left to right and include normal heart tube looping (class I), impaired elongation of the cardiac cone to form the primitive heart tube (class II), incomplete fusion of bilateral heart fields (class III), cardia bifida (class IV) and a band-like distribution of myocardial cell precursors (class V). Numbers of embryos displaying each phenotype are noted in red for yolk^{sdc2MO} embryos and in blue for yolk$^{sdc2MO\ +\ sdc2\ mRNA}$ embryos. In rescued embryos, the percentage of embryos with cardiac anomalies decreased from 66% to 24% (P<0.01). (**J**) Bar graph depicting the spectrum of gut defects seen in yolk^{sdc2MO} embryos (red bars) and yolk^{sdc2MO} embryos co-injected with *sdc2* mRNA (blue bars) at 40 hpf. Below the graph, the expression of *foxa3* is shown in embryos displaying the spectrum of gut phenotypes seen in yolk^{sdc2MO} embryos (dorsal view, anterior up). From left to right, embryos display normal gut looping (white arrow) and asymmetric hepatic/pancreatic bud formation (black arrow), duplicated hepatic/pancreatic buds (black arrows), and bilateral condensation of the posterior endoderm resulting in the formation of a two-sided foregut (white arrows).

4% incidence of right-sided heart looping, which is similar to the rate of heart reversal in uninjected wild-type embryos. The normal cardiac development in yolk^{sptMO} embryos is striking when compared with traditional *spt* morphants, in which injection of only 3 ng of morpholino per embryo yields a high percentage of left-right cardiac patterning defects (Amack et al., 2007; Bisgrove et al., 2000). These results highlight the fact that the yolk forms a functionally distinct compartment from the embryo, that yolk expression of Spt is not necessary for early heart development, and that *spt* morpholino injected into the yolk at the dome stage does not inhibit known *spt* gene functions in embryonic cells, consistent with the observation that the yolk^{MO} injection does not label embryonic cells (Fig. 1H).

To assess whether the cardia bifida phenotypes seen in yolk^{sdc2MO} embryos are specific to the function of Sdc or are due in part to off-target effects of the morpholinos, rescue experiments were performed by co-injecting *sdc2* MO(SB) and *sdc2* mRNA into embryos at the dome stage. In the rescue experiments, the percentage of yolk^{sdc2MO} embryos with cardiac anomalies decreased from 66% (n=270) to 24% (n=358, P<0.01) and the cardiac defects tended towards the milder end of the spectrum, i.e. incomplete heart-field fusion and impaired primitive heart tube formation (Fig. 2I). The ability to rescue the severe cardia bifida phenotypes in yolk^{sdc2MO} embryos indicates that these phenotypes are attributable to the loss of extra-embryonic Sdc.

In addition to the cardiac migration defects seen in yolk^{sdc2MO} embryos, gut migration abnormalities were also observed. In wild-type embryos, posterior endoderm condenses into a single rod-like structure along the midline to form the foregut by 24 hpf (Field et al., 2003). Subsequently, there is asymmetric development of the liver and pancreas buds off the foregut (Ober et al., 2003). The foregut marker *foxa3* was expressed in all yolk^{sdc2MO} embryos, indicating that gut primordia specification was normal. However, over 43% (25/58) of yolk^{sdc2MO} embryos had foregut abnormalities at 40 hpf, consistent with defects in gut primordia migration. Foregut anomalies included duplicated hepatic/pancreatic buds and bilateral condensation of the posterior endoderm, resulting in the formation of a two-sided foregut (Fig. 2J). The bifid gut phenotypes seen in

yolk^{sdc2MO} embryos are specific to the function of extra-embryonic *sdc2*, as co-injection of *sdc2* MO(SB) and *sdc2* mRNA into the dome stage resulted in normal gut formation in 95% (58/61) of embryos, indicating a 10-fold rescue of gut development by the expression of *sdc2* in the yolk.

These results indicate that migration of the embryonic heart and gut primordia depends specifically on the function of Sdc2 in the YSL. Strikingly, endogenously expressed *sdc2* in embryonic cells, including migrating heart and gut primordia, cannot functionally compensate for the loss of Sdc2 in the neighboring extra-embryonic YSL. Therefore, cardiac and gut cell migration is regulated in a non-cell-autonomous manner by extra-embryonic Sdc2.

Endoderm and endocardium are intact in yolk^{sdc2MO} embryos

Since the endoderm and endocardium are required for normal cardiac primordia migration (Alexander et al., 1998; David and Rosa, 2001; Holtzman et al., 2007), we examined yolk^{sdc2MO} embryos for abnormalities in these cell types. Expression of the early endodermal marker *sox17* was normal in yolk^{sdc2MO} embryos (n=20, data not shown). Endocardium development, as assessed by GFP expression, in yolk^{sdc2MO} *Tg(fli1:GFP)* embryos was also normal (n=24 embryos) to the extent detectable with the transgene *Tg(fli1:GFP)*. This suggests that cardiac and gut bifida phenotypes in yolk^{sdc2MO} embryos are not due to defects in endoderm or endocardium development.

Extra-embryonic Sdc2 is required for basement membrane formation, cardiomyocyte polarity and fibrillogenesis throughout the embryo

Myocardial and foregut primordia form sheets of polarized epithelia that adhere to and migrate on key components within the extracellular matrix. A number of molecules provide crucial links between extracellular structures and the cytoskeleton to facilitate epithelial polarization and migration. Laminin is found within the basement membrane and required for the induction of cell polarity that leads to the organization of embryonic tissues (Li et al., 2003; Yarnitzky and Volk, 1995). In CHO cells, Sdc2 is required for assembly of laminin into a fibrillar matrix in vitro (Klass et al., 2000). To investigate whether the basement membrane and cardiomyocyte polarity are altered in yolk^{sdc2MO} embryos, transverse sections of 20- to 22-somite-stage embryos were immunostained for laminin and atypical protein kinase C (aPKC). In wild-type embryos, migrating cardiomyocytes and posterior endoderm had a strong apicolateral localization of aPKC (Fig. 3C,E), indicative of a well-organized polarized epithelium (Trinh and Stainier, 2004), and a clearly defined laminin matrix between the migrating cardiomyocytes and posterior endoderm (Fig. 3A). By contrast, cardiomyocytes in yolk^{sdc2MO} embryos had weak and disorganized aPKC staining, and posterior endoderm had little if any laminin staining (5/6 embryos; Fig. 3B,D,F). These results indicate that Sdc2 expressed in extra-embryonic YSL is required for cell polarity and laminin matrix formation in the basement membrane of cardiac and gut primordia.

Several lines of evidence support the requirement for fibronectin during cardiomyocyte precursor migration. Cardia bifida occurs in mutants with a disrupted *fibronectin 1* gene and in mutants with impaired fibronectin-cardiomyocyte interactions (Matsui et al., 2007; Sakaguchi et al., 2006; Trinh and Stainier, 2004). Mtx1 (also known as Mxtx1), a YSL-specific transcription factor, controls *fibronectin 1* transcription in a non-cell-autonomous manner and its knockdown causes cardia bifida (Sakaguchi et al., 2006). To investigate whether extra-embryonic *sdc2* also impacts fibronectin

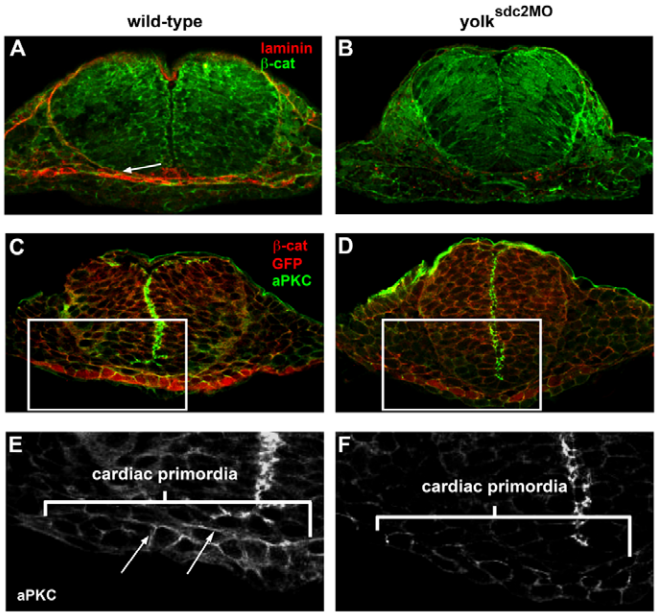

Fig. 3. Basement membrane and epithelial cell polarity are disrupted in yolk^{sdc2MO} embryos. (**A**,**B**) Transverse sections of wild-type (A) and yolk^{sdc2MO} (B) embryos at 22 somites reveal laminin deposition (white arrow) between the cardiac and ventral foregut primordia in wild-type embryos (3/3) and reduced laminin in yolk^{sdc2MO} embryos (5/6). Laminin, red; β-catenin, green. (**C-F**) Transverse sections of *Tg(cmlc2:GFP)* embryos at 22 somites immunostained for the cell-junction protein aPKC (green) and cardiac primordia (red). Magnified views of cardiac precursors (marked by rectangles in C and D) reveal apicolateral localization of aPKC protein (arrows) in noninjected embryos (E) and diminished aPKC in yolk^{sdc2MO} embryos (F).

fibrillogenesis, transverse sections of embryos at 20- to 22-somite stages were immunostained for fibronectin. Both uninjected controls and traditional *sdc2* morphants displayed normal fibronectin fibrillogenesis (n=16 and n=4 embryos, respectively; Fig. 4B,C). By contrast, many yolk^{sdc2MO} embryos completely lacked fibronectin fibril formation, not just at the YSL-embryo interface, but throughout the entire embryo (8/15 embryos; Fig. 4D). Fibronectin fibrillogenesis was rescued by co-injection of *sdc2* mRNA at the dome stage (17/20 embryos; Fig. 4E), whereas overexpression of *sdc2* in embryonic cells did not rescue fibrillogenesis in yolk^{sdc2MO} embryos (7/10 embryos; Fig. 4F).

mRNA encoding fibronectin is expressed in embryonic cells but not in the YSL, and the protein is secreted as monomers into the extracellular matrix, where fibrillogenesis occurs (Trinh and Stainier, 2004). Multiple mechanisms might lead to decreased fibronectin fibril formation, including diminished *fibronectin 1* mRNA expression, altered expression patterns of *fibronectin 1*, decreased levels of fibronectin monomer synthesis or secretion by embryonic cells, or loss of $\alpha_5\beta_1$ integrin, the major integrin in zebrafish that plays a crucial role in the initiation of fibronectin fibrillogenesis (Koshida et al., 2005; Mould et al., 2006). These possible mechanisms were systematically assessed in yolk^{sdc2MO} embryos. Levels of *fibronectin 1* mRNA were normal or slightly increased, with normal *fibronectin 1* expression patterns (Fig. 5A,B). The accumulation of fibronectin monomers was normal. Although fibronectin monomer secretion cannot be assessed in whole embryos, fibronectin protein synthesis and accumulation were normal in yolk^{sdc2MO} embryos (Fig. 5C). As a negative control, yolk^{mtx1MO} embryos were analyzed and found to have a significant

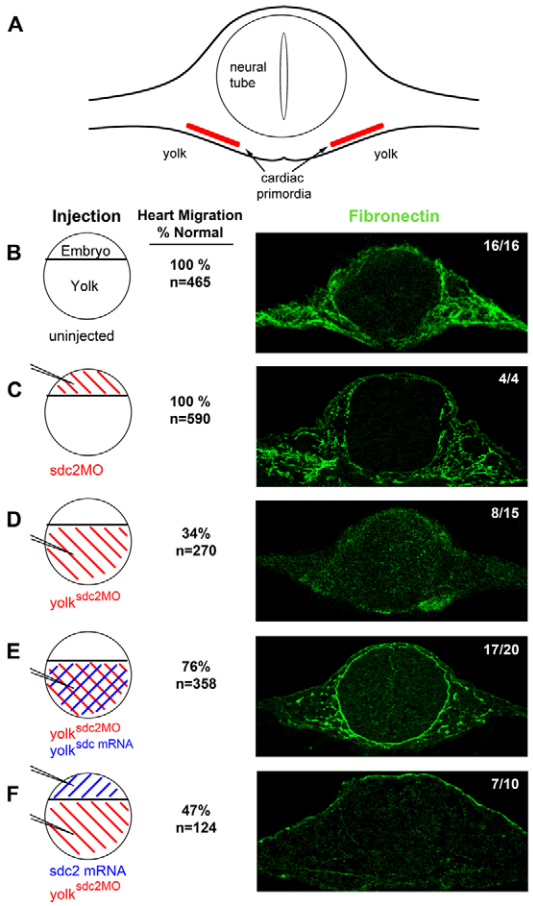

Fig. 4. Extra-embryonic Sdc2, but not embryonic Sdc2, is required for fibronectin fibrillogenesis throughout the embryo. (**A**) Diagram of an embryo cut in cross-section at the level of the cardiac primordia. Fibronectin fibrils form in the extracellular space adjacent to the cardiac primordia and surrounding the neural tube. (**B-F**) Transverse sections (right) of 22-somite embryos immunostained for fibronectin (green). Circular diagrams (left) represent different injection patterns of *sdc2* morpholino (red) and *sdc2* mRNA (blue). (B) Uninjected wild-type embryos (16/16 embryos) and (C) traditional *sdc2* morphants (4/4 embryos) had normal fibrillogenesis, indicating that embryonic Sdc2 is not required for fibrillogenesis. (D) yolk^{sdc2MO} morphants had no fibril formation in 8/15 embryos. With co-injection of *sdc2* mRNA into the yolk at the dome stage, fibrillogenesis was rescued in 17/20 embryos (E). By contrast, injection of *sdc2* mRNA at the 1-to-2-cell stage, to overexpress Sdc2 in embryonic cells, followed by injection of *sdc2* morpholino into yolk at the dome stage (F), did not rescue fibrillogenesis (7/10 embryos). As noted by the numbers adjacent to the confocal microscopy images, a higher percentage of normal cardiac migration correlates with the presence of fibronectin fibrils.

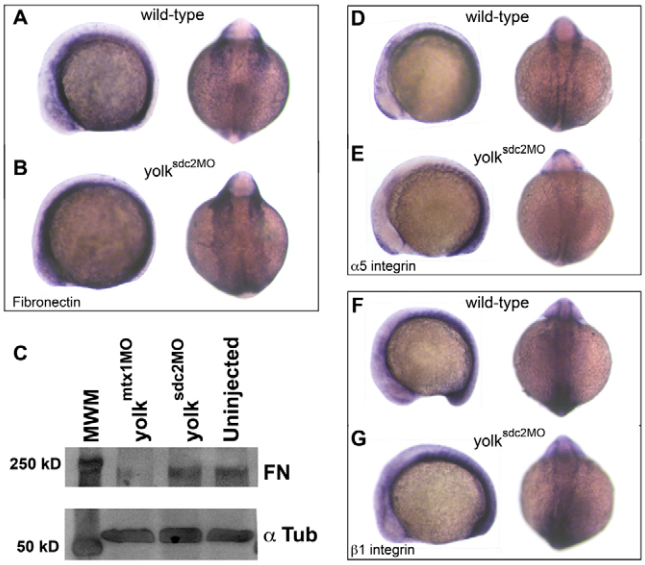

Fig. 5. Extra-embryonic Sdc2 controls fibronectin polymerization. (**A**,**B**) Lateral and dorsal views of wild-type (A) and yolk^{sdc2MO} (B) embryos at the 12-somite stage. *fibronectin 1* mRNA expression patterns were normal in yolk^{sdc2MO} embryos. (**C**) Western blot experiment showing normal accumulation of fibronectin (FN) protein monomers in wild-type and yolk^{sdc2MO} embryos. yolk^{mtx1MO} embryos have decreased fibronectin monomer accumulation due to decreased transcription of *fibronectin 1* (Sakaguchi et al., 2006). α-tubulin (α Tub) was used as a loading control. (**D-G**) Lateral and dorsal views of wild-type (D,F) and yolk^{sdc2MO} (E,G) embryos at the 12-somite stage reveal similar expression patterns for mRNA encoding α5 integrin (D,E) and β1 integrin (F,G).

reduction in the accumulation of fibronectin monomers, as previously reported (Sakaguchi et al., 2006). Expression patterns of RNA encoding α_5 and β_1 integrin in wild-type and yolk^{sdc2MO} embryos were found to be similar (Fig. 5D-G) and, using real-time PCR, integrin mRNA levels (relative to β actin, Bactin2) in yolk^{sdc2MO} embryos were found to be similar to wild-type embryos (0.7:1). Therefore, it appears that extra-embryonic Sdc2 is not required for fibronectin biosynthesis or for the expression of the major fibronectin receptor $\alpha_5\beta_1$ integrin, but is required for the polymerization of fibronectin monomers into complex fibrils throughout the embryo.

Role of extra-embryonic Sdc2 is distinct from Mtx1

Sakaguchi et al. (Sakaguchi et al., 2006) described similar, although less severe, cardiac and foregut anomalies in zebrafish with knockdown of the YSL-specific transcription factor Mtx1. By an unknown mechanism, extra-embryonic Mtx1 controls *fibronectin 1* transcription in a non-cell-autonomous manner. Despite the phenotypic similarities between yolk^{sdc2MO} and yolk^{mtx1MO} embryos, no apparent genetic interaction exists between Sdc2 and Mtx1. In contrast to *mtx1* knockdown, *sdc2* knockdown does not affect *fibronectin 1* mRNA expression or fibronectin protein accumulation (Fig. 5) but instead it impairs fibronectin matrix assembly (Fig. 4). In addition, knockdown of extra-embryonic *mtx1* does not alter *sdc2* mRNA expression (data not shown). As a functional test, cardiac migration defects were seen in 50% of yolk^{mtx1MO} embryos (n=39) and the aberrant cardiac migration was not rescued by coexpression of *sdc2* mRNA (65% with cardiac migration defects, n=54). Together, these results indicate that there are multiple genetic pathways in nonembryonic cells that control embryonic development and cardiac primordia migration, one of which involves induction of extracellular matrix formation at the YSL-embryo interface by extra-embryonic Sdc2.

Cleavage/shedding of extra-embryonic Sdc2 is not required for fibrillogenesis and organogenesis

The syndecan family of proteoglycans has a juxtamembrane cleavage site that allows release of the N-terminal ectodomain into the extracellular space in a process known as proteoglycan shedding (Fears et al., 2006). This process presumably allows the ectodomain

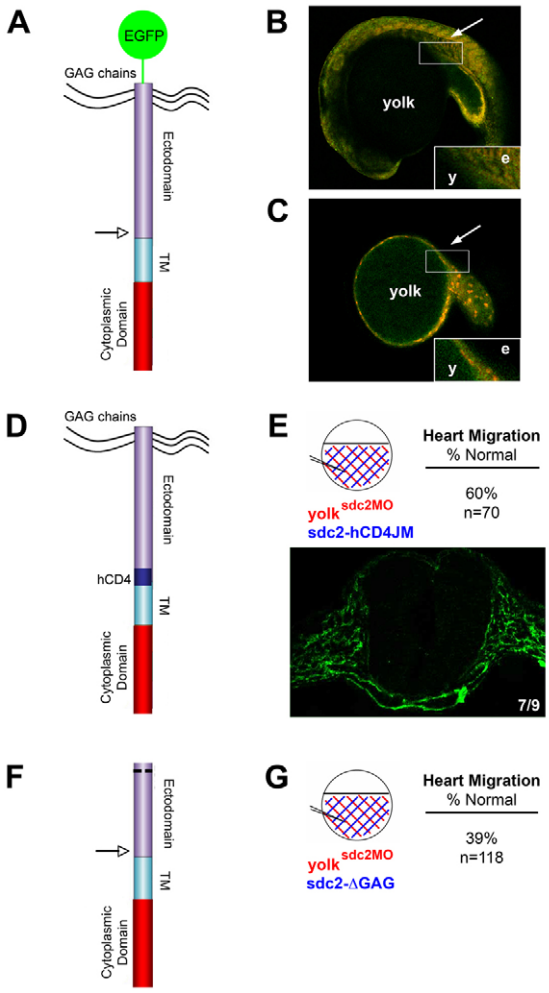

Fig. 6. Non-shed extra-embryonic Sdc2 is sufficient for embryonic organ primordia migration and fibrillogenesis. (**A**) Schematic of the *GFP-sdc2* construct with an arrow marking the location of the putative juxtamembrane cleavage site. TM, transmembrane domain. (**B**,**C**) Confocal microscopy images reveal GFP (green) expression in embryonic tissue (arrow) with injection of the *GFP-sdc2* construct at the single-cell stage (B) but restriction of GFP expression to the YSL/yolk in embryos (*n*=10) injected at the dome stage (C; arrow shows where embryonic tissue is located). The distribution of co-injected rhodamine-tagged control morpholino (red) correlates with the GFP expression. Insets in B and C show GFP distribution at higher magnification. e, embryo; y, yolk. (**D**) Schematic of the *sdc2-hCD4JM* construct. In this construct, 15 juxtamembrane amino acids, including the putative cleavage sequence for proteoglycan shedding, were replaced with a noncleavable sequence from the juxtamembrane domain of human CD4 (hCD4). (**E**) Co-injection of *sdc2* morpholino and *sdc2-hCD4JM* mRNA into yolk at the dome stage (injection pattern shown in the circular diagram) rescued fibronectin fibrillogenesis in 7/9 embryos (fibronectin fibrils in green) and cardiac migration in 60% of embryos (*n*=70). (**F**) Schematic of the *sdc2-ΔGAG* construct that contains the N-terminal membrane localization sequence but lacks all GAG attachment sites. (**G**) In contrast to *sdc2-hCD4JM*, co-injection of *sdc2* morpholino and *sdc2-ΔGAG* mRNA into the yolk at the dome stage did not rescue cardiac primordia migration (normal in only 39% of embryos, *n*=118).

to function at a distance from the cell in which it is synthesized. First, to detect whether the Sdc2 ectodomain moves a long distance from YSL into the regions in which fibrillogenesis is rescued by YSL-

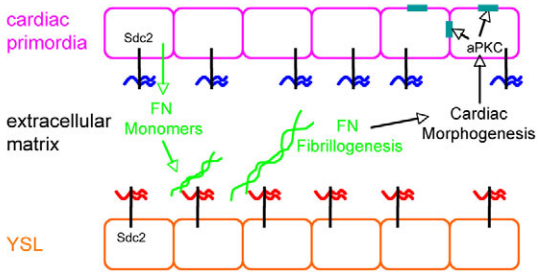

Fig. 7. Model of Sdc2 function during early organ formation. Sdc2 core protein (black) is expressed in both embryonic and extra-embryonic tissues. Fibronectin (FN) monomers are secreted by embryonic cells and require extra-embryonic Sdc2 GAG chains (red) to form FN fibrils (green strands). Once FN polymerization is initiated at the YSL-embryo interface, fibrillogenesis subsequently spreads throughout the embryo, mediating epithelial cell polarization, intracellular localization of aPKC (cyan bars) and cardiac cell migration. Strikingly, embryonically expressed Sdc2, with presumably distinct GAG chains (blue), is not capable of rescuing fibrillogenesis in the absence of extra-embryonic Sdc2 function. Laminin matrix formation by extra-embryonic Sdc2 might serve a similar function in gut cell migration.

expressed *sdc2*, a construct was made with GFP tagged to the ectodomain of Sdc2, N-terminal to the juxtamembrane proteolytic cleavage site (Fig. 6A). With release of the ectodomain from the cell surface by 'shedding', GFP would presumably move away from its cell of origin. Confocal microscopy images of embryos with *GFP-sdc2* mRNA injected into the yolk at the dome stage revealed that GFP fluorescence was concentrated within and around the YSL (Fig. 6C), and was not detected deeply in embryonic tissues (arrow in Fig. 6C), where fibrillogenesis is altered by knockdown of *sdc2* in extra-embryonic cells. At the level of resolution afforded by confocal microscopy, these results indicate that the GFP-tagged Sdc2 ectodomain expressed in the YSL did not move deeply into embryonic tissues. These experiments do not address whether endogenous Sdc2 is cleaved and moves a short distance from the source. Confinement of GFP-labeled Sdc2 near the YSL could be due to a lack of cleavage/shedding or to retention of the cleaved Sdc2 ectodomain at the cell surface by interaction of Sdc2 GAGs with the surrounding extracellular matrix. As a control to assess whether GFP-labeled Sdc2 could be detected in embryonic tissues, *GFP-sdc2* mRNA was injected at the 1-to-2-cell stage and resulted in GFP expression throughout the embryo (arrow in Fig. 6B).

To functionally test whether cleavage/shedding of extra-embryonic Sdc2 is necessary for fibrillogenesis and organ primordia movement, we generated a noncleavable Sdc2 construct (*sdc2-hCD4JM*) (Fig. 6D), in which the juxtamembrane cleavage sequence was replaced with noncleavable sequence from human CD4 (Wang et al., 2005). Strikingly, expression of *sdc2-hCD4JM* in yolk^{sdc2MO} embryos was able to rescue heart migration and fibrillogenesis throughout the embryo (Fig. 6E), similar to wild-type *sdc2* (Fig. 4E). These results indicate that shedding is not necessary for extra-embryonic Sdc2 function, and that Sdc2 tethered to the plasma membrane of the extra-embryonic YSL is capable of driving fibrillogenesis and cell migration throughout the embryo.

Syndecan 2 GAG chains are required for fibrillogenesis

We propose a model in which extra-embryonic Sdc2 functions to drive extracellular matrix assembly and organ primordia movement within the embryo (Fig. 7). Sdc2 is expressed in both embryonic and extra-

embryonic tissues, but the two forms of Sdc2 are functionally distinct. In syndecan 4, a homolog of Sdc2, the GAG chains interact with the heparin-binding domains of fibronectin (Carey, 1997; Klass et al., 2000; Whiteford et al., 2007). Hence, one exciting possibility is that specific GAG chain modifications on extra-embryonic Sdc2 (red in Fig. 7) drive fibrillogenesis, and these GAG chain modifications are distinct from those found on Sdc2 expressed in embryonic cells (blue in Fig. 7), which are incapable of driving fibrillogenesis, but perform other functions. In support of this hypothesis, cardiac migration defects are not rescued in yolk^{sdc2MO} embryos by co-injection of *sdc2-ΔGAG*, an Sdc2 construct lacking GAG attachment sites (Fig. 6F,G). These results demonstrate that Sdc2 GAG chains are crucial for cardiac primordia migration and suggest that GAG chain modifications vary from one embryonic compartment to another, leading to differences in proteoglycan function.

DISCUSSION

Sdc2 is a transmembrane heparan sulfate proteoglycan with heparan sulfate glycosaminoglycan (GAG) chains covalently bound to its ectodomain, and is expressed in both embryonic and extra-embryonic cells during zebrafish development. The roles of extra-embryonic cells, including the extra-embryonic yolk syncytial layer (YSL), in zebrafish are poorly understood. Here we present evidence indicating that extra-embryonic Sdc2 cell-autonomously directs fibronectin fibrillogenesis and laminin matrix assembly at the YSL-embryo interface, and non-cell-autonomously controls matrix formation, and cardiac and gut primordia movement throughout the embryo.

Given that *sdc2* mRNA is expressed throughout the embryo, it is striking that neither endogenous embryonic Sdc2 nor overexpression of *sdc2* mRNA throughout the embryo by injection of the mRNA at the single-cell stage can compensate for the loss of Sdc2 in extra-embryonic cells (see Fig. 4). Further evidence for a functional difference between embryonic and extra-embryonic Sdc2 comes from traditional morphant studies in which knockdown of *sdc2* in embryonic cells alters angiogenesis (Chen et al., 2004) and left-right patterning (data not shown) but does not lead to a bifid heart or gut. Although it is possible that extra-embryonic Sdc2 modulates a signal in the YSL that induces secretion of an unknown signal out of the YSL into the embryo to mediate fibrillogenesis, cell polarization and cell migration in the embryo, or that extra-embryonic Sdc2 plays a role in yolk syncytial nuclei movement that somehow modulates cardiac primordia patterning (Carvalho et al., 2009), a more parsimonious explanation is that extra-embryonic Sdc2 directly controls fibrillogenesis at the YSL-embryo interface and subsequently controls cell migration. The ability of YSL-expressed Sdc2 to nucleate fibrillogenesis concurs with the role of syndecans in promoting fibrillogenesis in cell culture (Carey, 1997; Klass et al., 2000; Woods and Couchman, 1998). Although ectodomain shedding in extra-embryonic Sdc2 does not appear to be necessary for fibronectin polymerization, extra-embryonic GAG chains attached to Sdc2 appear to be required for organ primordia migration (Fig. 6). Overall, our results indicate that functional differences exist between embryonic and extra-embryonic Sdc2 and that these differences are at least in part driven by GAG chains on Sdc2. An intriguing possibility is it that the fine structural modifications of the GAG chains attached to Sdc2 in the extra-embryonic cells are distinct from the fine structural modifications of the GAG chains attached to Sdc2 in embryonic cells (Fig. 7).

The striking foregut anomalies observed in yolk^{sdc2MO} embryos are not observed in *natter* (*fibronectin 1*) mutants (Trinh and Stainier, 2004), suggesting that foregut migration is not dependent on fibronectin fibrillogenesis and that Sdc2 utilizes some other non-cell-autonomous mechanism to control gut epithelial migration. Members of the laminin family are required for basement membrane assembly. Basement membranes are specialized extracellular matrices that form sheets underlying cell layers and play a crucial role in cell polarization and tissue epithelialization (Li et al., 2003; Yarnitzky and Volk, 1995). In zebrafish, a basement membrane is located between the cardiac primordia and ventral foregut primordia. As assayed by laminin and aPKC immunoreactivity, this basement membrane is nearly absent and epithelial cell polarity is disrupted in yolk^{sdc2MO} embryos (see Fig. 3). Interestingly, similar basement membrane, cell polarity and gut migration defects occur in both yolk^{sdc2MO} and yolk^{mtx1MO} embryos, suggesting that posterior endoderm migration may depend on the formation of an organized basement membrane (Sakaguchi et al., 2006). Additional evidence supporting this hypothesis comes from zebrafish *has* (*prkci*) mutants that lack aPKC (Horne-Badovinac et al., 2001). A deficiency in aPKC results in impaired formation of the zonula adherens in the polarized epithelia of the digestive tract, and leads to gut malformations including duplication of the hepatic/pancreatic buds.

In summary, extra-embryonic Sdc2 appears to direct heart and gut primordia migration by initiating fibronectin and laminin matrix assembly at the yolk-embryo interface. Strikingly, fibrillogenesis spreads throughout the entire zebrafish embryo. Functional differences in GAG chain structure between embryonic and extra-embryonic Sdc2 might serve to regulate fibrillogenesis, cell migration and epithelial morphogenesis of multiple organ systems throughout the embryo.

Acknowledgements

We thank M. L. Condic for comments on the manuscript, and members of the Yost lab for insightful discussions. This research was supported by grants from the NHLBI (HL075472) and Primary Children's Medical Foundation to H.J.Y. C.B.A. was supported in part by the Children's Health Research Center at the University of Utah. Deposited in PMC for release after 12 months.

Supplementary material

Supplementary material for this article is available at
http://dev.biologists.org/cgi/content/full/136/18/3143/DC1

References

Akiyama, S. K., Yamada, S. S., Chen, W. T. and Yamada, K. M. (1989). Analysis of fibronectin receptor function with monoclonal antibodies: roles in cell adhesion, migration, matrix assembly, and cytoskeletal organization. *J. Cell Biol.* **109**, 863-875.

Alexander, J. and Stainier, D. Y. (1999). A molecular pathway leading to endoderm formation in zebrafish. *Curr. Biol.* **9**, 1147-1157.

Alexander, J., Stainier, D. Y. and Yelon, D. (1998). Screening mosaic F1 females for mutations affecting zebrafish heart induction and patterning. *Dev. Genet.* **22**, 288-299.

Alexander, J., Rothenberg, M., Henry, G. L. and Stainier, D. Y. (1999). casanova plays an early and essential role in endoderm formation in zebrafish. *Dev. Biol.* **215**, 343-357.

Amack, J. D. and Yost, H. J. (2004). The T box transcription factor no tail in ciliated cells controls zebrafish left-right asymmetry. *Curr. Biol.* **14**, 685-690.

Amack, J. D., Wang, X. and Yost, H. J. (2007). Two T-box genes play independent and cooperative roles to regulate morphogenesis of ciliated Kupffer's vesicle in zebrafish. *Dev. Biol.* **310**, 196-210.

Bischof, J. and Driever, W. (2004). Regulation of hhex expression in the yolk syncytial layer, the potential Nieuwkoop center homolog in zebrafish. *Dev. Biol.* **276**, 552-562.

Bisgrove, B. W., Essner, J. J. and Yost, H. J. (2000). Multiple pathways in the midline regulate concordant brain, heart and gut left-right asymmetry. *Development* **127**, 3567-3579.

Brand, T. (2003). Heart development: molecular insights into cardiac specification and early morphogenesis. *Dev. Biol.* **258**, 1-19.

Bultmann, H., Santas, A. J. and Peters, D. M. (1998). Fibronectin fibrillogenesis involves the heparin II binding domain of fibronectin. *J. Biol. Chem.* **273**, 2601-2609.

Carey, D. J. (1997). Syndecans: multifunctional cell-surface co-receptors. *Biochem. J.* **327**, 1-16.

Carvalho, L., Stuhmer, J., Bois, J. S., Kalaidzidis, Y., Lecaudey, V. and Heisenberg, C. P. (2009). Control of convergent yolk syncytial layer nuclear movement in zebrafish. *Development* **136**, 1305-1315.
Chen, E., Hermanson, S. and Ekker, S. C. (2004). Syndecan-2 is essential for angiogenic sprouting during zebrafish development. *Blood* **103**, 1710-1719.
Chen, J. N., Haffter, P., Odenthal, J., Vogelsang, E., Brand, M., van Eeden, F. J., Furutani-Seiki, M., Granato, M., Hammerschmidt, M., Heisenberg, C. P. et al. (1996). Mutations affecting the cardiovascular system and other internal organs in zebrafish. *Development* **123**, 293-302.
Chen, S. and Kimelman, D. (2000). The role of the yolk syncytial layer in germ layer patterning in zebrafish. *Development* **127**, 4681-4689.
Christopher, R. A., Kowalczyk, A. P. and McKeown-Longo, P. J. (1997). Localization of fibronectin matrix assembly sites on fibroblasts and endothelial cells. *J. Cell Sci.* **110**, 569-581.
Chung, C. Y. and Erickson, H. P. (1997). Glycosaminoglycans modulate fibronectin matrix assembly and are essential for matrix incorporation of tenascin-C. *J. Cell Sci.* **110**, 1413-1419.
D'Amico, L. A. and Cooper, M. S. (2001). Morphogenetic domains in the yolk syncytial layer of axiating zebrafish embryos. *Dev. Dyn.* **222**, 611-624.
David, N. B. and Rosa, F. M. (2001). Cell autonomous commitment to an endodermal fate and behaviour by activation of Nodal signalling. *Development* **128**, 3937-3947.
Dickmeis, T., Mourrain, P., Saint-Etienne, L., Fischer, N., Aanstad, P., Clark, M., Strahle, U. and Rosa, F. (2001). A crucial component of the endoderm formation pathway, CASANOVA, is encoded by a novel sox-related gene. *Genes Dev.* **15**, 1487-1492.
Dzamba, B. J., Bultmann, H., Akiyama, S. K. and Peters, D. M. (1994). Substrate-specific binding of the amino terminus of fibronectin to an integrin complex in focal adhesions. *J. Biol. Chem.* **269**, 19646-19652.
Fears, C. Y., Gladson, C. L. and Woods, A. (2006). Syndecan-2 is expressed in the microvasculature of gliomas and regulates angiogenic processes in microvascular endothelial cells. *J. Biol. Chem.* **281**, 14533-14536.
Field, H. A., Ober, E. A., Roeser, T. and Stainier, D. Y. (2003). Formation of the digestive system in zebrafish. I. Liver morphogenesis. *Dev. Biol.* **253**, 279-290.
Fogerty, F. J., Akiyama, S. K., Yamada, K. M. and Mosher, D. F. (1990). Inhibition of binding of fibronectin to matrix assembly sites by anti-integrin (alpha 5 beta 1) antibodies. *J. Cell Biol.* **111**, 699-708.
Glickman, N. S. and Yelon, D. (2002). Cardiac development in zebrafish: coordination of form and function. *Semin. Cell Dev. Biol.* **13**, 507-513.
Hocking, D. C., Sottile, J. and McKeown-Longo, P. J. (1994). Fibronectin's III-1 module contains a conformation-dependent binding site for the amino-terminal region of fibronectin. *J. Biol. Chem.* **269**, 19183-19187.
Holtzman, N. G., Schoenebeck, J. J., Tsai, H. J. and Yelon, D. (2007). Endocardium is necessary for cardiomyocyte movement during heart tube assembly. *Development* **134**, 2379-2386.
Horne-Badovinac, S., Lin, D., Waldron, S., Schwarz, M., Mbamalu, G., Pawson, T., Jan, Y., Stainier, D. Y. and Abdelilah-Seyfried, S. (2001). Positional cloning of heart and soul reveals multiple roles for PKC lambda in zebrafish organogenesis. *Curr. Biol.* **11**, 1492-1502.
Horne-Badovinac, S., Rebagliati, M. and Stainier, D. Y. (2003). A cellular framework for gut-looping morphogenesis in zebrafish. *Science* **302**, 662-665.
Huang, C. J., Tu, C. T., Hsiao, C. D., Hsieh, F. J. and Tsai, H. J. (2003). Germ-line transmission of a myocardium-specific GFP transgene reveals critical regulatory elements in the cardiac myosin light chain 2 promoter of zebrafish. *Dev. Dyn.* **228**, 30-40.
Kawahara, A., Nishi, T., Hisano, Y., Fukui, H., Yamaguchi, A. and Mochizuki, N. (2009). The sphingolipid transporter spns2 functions in migration of zebrafish myocardial precursors. *Science* **323**, 524-527.
Kikuchi, Y., Trinh, L. A., Reiter, J. F., Alexander, J., Yelon, D. and Stainier, D. Y. (2000). The zebrafish bonnie and clyde gene encodes a Mix family homeodomain protein that regulates the generation of endodermal precursors. *Genes Dev.* **14**, 1279-1289.
Kimmel, C. B. and Law, R. D. (1985). Cell lineage of zebrafish blastomeres. II. Formation of the yolk syncytial layer. *Dev. Biol.* **108**, 86-93.
Kimmel, C. B., Ballard, W. W., Kimmel, S. R., Ullmann, B. and Schilling, T. F. (1995). Stages of embryonic development of the zebrafish. *Dev. Dyn.* **203**, 253-310.
Klass, C. M., Couchman, J. R. and Woods, A. (2000). Control of extracellular matrix assembly by syndecan-2 proteoglycan. *J. Cell Sci.* **113**, 493-506.
Koshida, S., Kishimoto, Y., Ustumi, H., Shimizu, T., Furutani-Seiki, M., Kondoh, H. and Takada, S. (2005). Integrinalpha5-dependent fibronectin accumulation for maintenance of somite boundaries in zebrafish embryos. *Dev. Cell* **8**, 587-598.
Kramer, K. L. and Yost, H. J. (2002). Ectodermal syndecan-2 mediates left-right axis formation in migrating mesoderm as a cell-nonautonomous Vg1 cofactor. *Dev. Cell* **2**, 115-124.
Kupperman, E., An, S., Osborne, N., Waldron, S. and Stainier, D. Y. (2000). A sphingosine-1-phosphate receptor regulates cell migration during vertebrate heart development. *Nature* **406**, 192-195.
Lawson, N. D. and Weinstein, B. M. (2002). In vivo imaging of embryonic vascular development using transgenic zebrafish. *Dev. Biol.* **248**, 307-318.
LeBaron, R. G., Esko, J. D., Woods, A., Johansson, S. and Hook, M. (1988). Adhesion of glycosaminoglycan-deficient chinese hamster ovary cell mutants to fibronectin substrata. *J. Cell Biol.* **106**, 945-952.
Li, S., Edgar, D., Fassler, R., Wadsworth, W. and Yurchenco, P. D. (2003). The role of laminin in embryonic cell polarization and tissue organization. *Dev. Cell* **4**, 613-624.
Li, S., Zhou, D., Lu, M. M. and Morrisey, E. E. (2004). Advanced cardiac morphogenesis does not require heart tube fusion. *Science* **305**, 1619-1622.
Linask, K. K. and Lash, J. W. (1988). A role for fibronectin in the migration of avian precardiac cells. I. Dose-dependent effects of fibronectin antibody. *Dev. Biol.* **129**, 315-323.
Matsui, T., Raya, A., Callol-Massot, C., Kawakami, Y., Oishi, I., Rodriguez-Esteban, C. and Belmonte, J. C. (2007). miles-apart-Mediated regulation of cell-fibronectin interaction and myocardial migration in zebrafish. *Nat. Clin. Pract. Cardiovasc. Med.* **4** Suppl. **1**, S77-S82.
McDonald, J. A., Quade, B. J., Broekelmann, T. J., LaChance, R., Forsman, K., Hasegawa, E. and Akiyama, S. (1987). Fibronectin's cell-adhesive domain and an amino-terminal matrix assembly domain participate in its assembly into fibroblast pericellular matrix. *J. Biol. Chem.* **262**, 2957-2967.
McFadden, D. G. and Olson, E. N. (2002). Heart development: learning from mistakes. *Curr. Opin. Genet. Dev.* **12**, 328-335.
Mould, A. P., McLeish, J. A., Huxley-Jones, J., Goonesinghe, A. C., Hurlstone, A. F., Boot-Handford, R. P. and Humphries, M. J. (2006). Identification of multiple integrin beta1 homologs in zebrafish (*Danio rerio*). *BMC Cell Biol.* **7**, 24.
Nasevicius, A. and Ekker, S. C. (2000). Effective targeted gene 'knockdown' in zebrafish. *Nat. Genet.* **26**, 216-220.
Ober, E. A. and Schulte-Merker, S. (1999). Signals from the yolk cell induce mesoderm, neuroectoderm, the trunk organizer, and the notochord in zebrafish. *Dev. Biol.* **215**, 167-181.
Ober, E. A., Field, H. A. and Stainier, D. Y. (2003). From endoderm formation to liver and pancreas development in zebrafish. *Mech. Dev.* **120**, 5-18.
Odenthal, J. and Nusslein-Volhard, C. (1998). fork head domain genes in zebrafish. *Dev. Genes Evol.* **208**, 245-258.
Osborne, N., Brand-Arzamendi, K., Ober, E. A., Jin, S. W., Verkade, H., Holtzman, N. G., Yelon, D. and Stainier, D. Y. (2008). The spinster homolog, two of hearts, is required for sphingosine 1-phosphate signaling in zebrafish. *Curr. Biol.* **18**, 1882-1888.
Roberts, D. J. (2000). Molecular mechanisms of development of the gastrointestinal tract. *Dev. Dyn.* **219**, 109-120.
Rohr, S., Bit-Avragim, N. and Abdelilah-Seyfried, S. (2006). Heart and soul/PRKCi and nagie oko/Mpp5 regulate myocardial coherence and remodeling during cardiac morphogenesis. *Development* **133**, 107-115.
Rosenquist, G. C. (1970). Cardia bifida in chick embryos: anterior and posterior defects produced by transplanting tritiated thymidine-labeled grafts medial to the heart-forming regions. *Teratology* **3**, 135-142.
Rupp, R. A., Snider, L. and Weintraub, H. (1994). *Xenopus* embryos regulate the nuclear localization of XMyoD. *Genes Dev.* **8**, 1311-1323.
Sakaguchi, T., Kikuchi, Y., Kuroiwa, A., Takeda, H. and Stainier, D. Y. (2006). The yolk syncytial layer regulates myocardial migration by influencing extracellular matrix assembly in zebrafish. *Development* **133**, 4063-4072.
Schwarzbauer, J. E. (1991). Identification of the fibronectin sequences required for assembly of a fibrillar matrix. *J. Cell Biol.* **113**, 1463-1473.
Sechler, J. L., Corbett, S. A. and Schwarzbauer, J. E. (1997). Modulatory roles for integrin activation and the synergy site of fibronectin during matrix assembly. *Mol. Biol. Cell* **8**, 2563-2573.
Stainier, D. Y. (2001). Zebrafish genetics and vertebrate heart formation. *Nat. Rev. Genet.* **2**, 39-48.
Stainier, D. Y. (2005). No organ left behind: tales of gut development and evolution. *Science* **307**, 1902-1904.
Stainier, D. Y., Fouquet, B., Chen, J. N., Warren, K. S., Weinstein, B. M., Meiler, S. E., Mohideen, M. A., Neuhauss, S. C., Solnica-Krezel, L., Schier, A. F. et al. (1996). Mutations affecting the formation and function of the cardiovascular system in the zebrafish embryo. *Development* **123**, 285-292.
Thisse, C., Thisse, B., Schilling, T. F. and Postlethwait, J. H. (1993). Structure of the zebrafish snail1 gene and its expression in wild-type, spadetail and no tail mutant embryos. *Development* **119**, 1203-1215.
Trinh, L. A. and Stainier, D. Y. (2004). Fibronectin regulates epithelial organization during myocardial migration in zebrafish. *Dev. Cell* **6**, 371-382.
Wang, Z., Gotte, M., Bernfield, M. and Reizes, O. (2005). Constitutive and accelerated shedding of murine syndecan-1 is mediated by cleavage of its core protein at a specific juxtamembrane site. *Biochemistry* **44**, 12355-12361.
Westerfield, M. (1994). *The Zebrafish Book*. Eugene, OR: University of Oregon Press.
Whiteford, J. R., Behrends, V., Kirby, H., Kusche-Gullberg, M., Muramatsu, T. and Couchman, J. R. (2007). Syndecans promote integrin-mediated adhesion of mesenchymal cells in two distinct pathways. *Exp. Cell Res.* **313**, 3902-3913.

Woods, A. and Couchman, J. R. (1998). Syndecans: synergistic activators of cell adhesion. *Trends Cell Biol.* **8**, 189-192.
Woods, A., Johansson, S. and Hook, M. (1988). Fibronectin fibril formation involves cell interactions with two fibronectin domains. *Exp. Cell Res.* **177**, 272-283.
Wu, C., Bauer, J. S., Juliano, R. L. and McDonald, J. A. (1993). The alpha 5 beta 1 integrin fibronectin receptor, but not the alpha 5 cytoplasmic domain, functions in an early and essential step in fibronectin matrix assembly. *J. Biol. Chem.* **268**, 21883-21888.
Yarnitzky, T. and Volk, T. (1995). Laminin is required for heart, somatic muscles, and gut development in the *Drosophila* embryo. *Dev. Biol.* **169**, 609-618.
Yelon, D. (2001). Cardiac patterning and morphogenesis in zebrafish. *Dev. Dyn.* **222**, 552-563.
Yelon, D., Horne, S. A. and Stainier, D. Y. (1999). Restricted expression of cardiac myosin genes reveals regulated aspects of heart tube assembly in zebrafish. *Dev. Biol.* **214**, 23-37.
Zaffran, S. and Frasch, M. (2002). Early signals in cardiac development. *Circ. Res.* **91**, 457-469.